Macromolecules
ARTICLE

Macromolecules **2010**, *43*, 4573–4583 **4573**
DOI: 10.1021/ma100453d

Clarifying the Mechanism of the Denisov Cycle: How do Hindered Amine Light Stabilizers Protect Polymer Coatings from Photo-oxidative Degradation?

Jennifer L. Hodgson and Michelle L. Coote*

Research School of Chemistry, Australian National University, Canberra, ACT 0200, Australia

Received February 26, 2010; Revised Manuscript Received April 16, 2010

ABSTRACT: Hindered amine light stabilizers (HALS) protect polymer coatings against photo-oxidative damage through the formation of nitroxide radicals, which subsequently consume damaging radical species in a process called the Denisov cycle. However, the exact mechanism for this process has been disputed, with a dozen different reaction pathways and over 30 individual reactions previously proposed in the literature. In this work, the full mechanism of the Denisov cycle is elucidated using high-level computational techniques for two different polymer systems. New intermediate species in the cycle have been postulated, and the final products determined. The nitroxide TEMPO can react either with the polymeric radical $^{\bullet}$R to form an alkoxyamine species >N−OR, with any available alkoxyl radicals $^{\bullet}$OR to form the oxyaminoether species $>N^{+}(O^{-})-OR$, or (more slowly) with the peroxyl radical $^{\bullet}$OOR to form the trioxide species >N−O−O−O−R. The alkoxyamine goes on to react with the peroxyl radical reforming the nitroxide along with ketone and alcohol products via a caged oxyaminoether and alkoxyl radical intermediate for polyethylene, and via either a caged oxyaminoether and alkoxyl radical intermediate or a caged aminoperoxylether and alkoxyl radical intermediate for polyester. The oxyaminoether undergoes an intramolecular hydrogen transfer reaction to form a hydroxylamine >N−OH and a ketone. The trioxide goes on to react with a secondary alcohol to form a hydroxylamine, a ketone and a hydroperoxide species via a concerted mechanism involving a six-membered ring transition state. The hydroxylamine species is then converted back to the corresponding nitroxide through hydrogen transfer to an alkyl, alkoxyl or peroxyl radical. A possible side reaction, reforming a HALS-type amine occurs through hydrogen donation to the aminyl radical product of the direct decomposition of the trioxide species into aminyl and hydroxyl radicals and dioxygen. This study will assist in the design of new and improved hindered amine light stabilizers for surface coatings.

Introduction

Polymer-coated steel products are widely used in the automotive and building industries, as well as in general household fittings and appliances. The polymer coating acts to protect the steel from corrosion as well as providing a colored and glossy finish to the surface. Generally, polymer topcoats are constructed of polyester or acrylic polymer chains that are networked into solid three-dimensional architectures by melamine formaldehyde or urethane-type cross-linkers.[1]

During prolonged exposure to sunlight and other weathering effects, polymer coatings undergo discolouration and become brittle, developing surface cracks. Numerous studies have attempted to identify and assess the degradation processes in the types of polymers used in coated steel applications.[2] The general mechanism of the photo-oxidative degradation of polymer systems is shown in reactions 1 to 4. Initiation is induced via the homolytic cleavage of polymeric bonds (R−R) by Norrish type I reactions, or by hydrogen abstraction by an atmospheric radical ($X^{\bullet}$) to form a polymeric radical ($R^{\bullet}$), which reacts with oxygen at a diffusion-controlled rate to form a peroxyl radical ($ROO^{\bullet}$).[3] Depending on the substitution pattern of R, the peroxyl radical may then abstract a hydrogen atom from the polymer backbone to form a hydroperoxide (ROOH), generating further alkyl radicals ($R^{\bullet}$).[4]

$$R-R \rightarrow R^{\bullet} + R^{\bullet} \quad (1)$$

$$RH + X^{\bullet} \rightarrow R^{\bullet} + XH \quad (2)$$

$$R^{\bullet} + O_2 \rightarrow ROO^{\bullet} \quad (3)$$

$$ROO^{\bullet} + RH \rightarrow ROOH + R^{\bullet} \quad (4)$$

Compounds including ultraviolet (UV) stabilizers are added to polymer coatings to protect the surface from light degradation. Although these additives can act through the direct absorption of UV radiation, one class of UV stabilizers, known as the hindered amine light stabilizers (HALS), are effective in the protection of surface coatings but do not absorb UV light. The mechanism by which this occurs has been the subject of several prior investigations. It was originally proposed that the activity of HALS was due entirely to their ability to scavenge radicals via the formation of nitroxide radicals, through a process known as the Denisov cycle.[2] More recently, other protection mechanisms which do not involve the Denisov cycle have been suggested, including the thermal regeneration of the nitroxide through the bond cleavage of alkoxyamines,[5] and the quenching of excited states of singlet oxygen, aliphatic carbonyls and aromatic hydrocarbons by hindered amines and nitroxides, thereby preventing initiation of photodegradation.[6]

A simplified mechanism of the Denisov cycle is shown in Scheme 1, with the HALS depicted as the six-membered heterocyclic amine 2,2,6,6-tetramethylpiperidine which is oxidized to the corresponding nitroxide radical, 2,2,6,6-tetramethylpiperidin-1-loxyl

*Corresponding author. E-mail: mcoote@rsc.anu.edu.au.

Published on Web 04/27/2010

Scheme 1. Simplified Mechanism of the Denisov Cycle, Showing Protection Using a Piperidine HALS (Where X is Typically H or an Alkyl Chain)

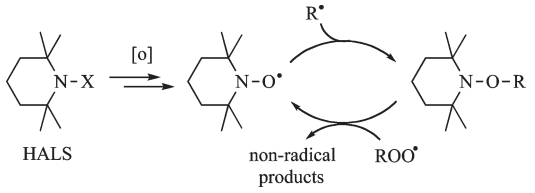

(TEMPO). This is thought to occur through an initial reaction with a hydroperoxide, which forms a hydroxylamine or alkoxyamine, with a subsequent oxidation by a radical such as a peroxyl radical forming the nitroxide.[7] Alternately, direct photo-oxidation of HALS by acylperoxyl radicals, formed by oxidation of a Norrish II photoylsis aldehyde product, has also been suggested.[8] The nitroxide subsequently reacts with an alkyl polymeric radical, R•, generated during photodegradation, to form an alkoxylamine. It has been observed in model systems that, after addition of the HALS, the nitroxide concentration grows (from zero) to a maximum value and then drops to level out at around 10% of the originally added HALS concentration, as nitroxides scavenge alkyl radicals to form alkoxyamines.[9] Additional experiments have also shown that when nitroxides are added directly to the polymer this same drop in concentration occurs,[10] and it is thought that alkoxyamines provide a reservoir of the HALS-stabilizing potential.[11,12] The alkoxyamine species then goes on to react with a peroxyl radical to reform the nitroxide as well as nonradical products. Therefore, the Denisov cycle acts in a catalytic fashion to transform both R• and ROO• radicals to nonradical species. The original Denisov mechanism for the reaction of the alkoxyamine and the peroxyl radical proposed that a polymeric product of the form ROOR is formed through transition state species of the form [> NO---R---OOR]‡.[2] However, this product has never been detected and has been discounted by a labeling study, which indicated that the nitroxide oxygen is exchanged for one of the peroxyl oxygen atoms during the reaction.[13]

Although HALS have been used commercially for many years, the correct mechanism by which nitroxides protect polymer coatings from photo-oxidative damage has been the subject of ongoing debate. Some of the key unanswered questions relate to how the peroxyl radical regenerates the nitroxide, and whether there are any side reactions that may account for the degradation of the protecting agent over time. In attempts to address these questions, at least a dozen different mechanistic pathways comprising over 30 individual reactions, have been proposed to contribute to or interfere with the Denisov cycle.[2,5,13−22] These are shown comprehensively in Schemes 2, 3 and 4, with the individual reactions labeled (5) to (33). The schemes show reactions involved in the scavenging of both polymeric and peroxyl radicals by nitroxides, and their conversion to nonradical products, with the subsequent regeneration of the nitroxide. Possible side reactions that may interfere with the catalytic cycle are also depicted.

Until now it has been difficult to distinguish between the various postulated mechanisms. However, due to the ease with which theoretical calculations can be used to study individual chemical reactions in such complicated reaction sequences, the various mechanisms suggested in the literature may easily be compared using computational methods in order to elucidate the most likely reaction mechanism. Previously, semiempirical and other low-level methods have been used to examine some of the possible reactions between peroxyl radicals and nitroxides[14] or alkoxyamines.[15,16] However, a comprehensive high-level *ab initio* study of all the proposed reactions in Schemes 2−4 has not been completed, and is described here for the first time. In this work the thermodynamics and kinetics of the reactions by which nitroxides interfere with polymer autoxidation will be quantitatively examined using previously established[23−26] accurate high-level computational chemistry methods in order to shed more light on the mechanisms of protection.

Theoretical Procedures

Standard *ab initio* molecular orbital[27] and density functional[28] calculations in this work were carried out using GAUSSIAN 03[29] and MOLPRO 2000.6.[30] Calculations on radicals were performed with an unrestricted wave function except in cases designated with an "R" prefix where a restricted open-shell wave function was used. Geometries of all species were fully optimized at the B3-LYP/6-31G(d) level of theory and frequencies were also calculated at this level and scaled by appropriate scale factors.[31] Transition state structures were verified by their (single) imaginary frequencies and by IRC calculations in the forward and reverse directions along the reaction paths. For all species, full systematic conformational searches (at a resolution of 120°) were carried out to ensure that global rather than merely local minima were located.

Improved energies for all reaction species were calculated at the G3(MP2)-RAD level.[32] This high-level composite method has been shown to deliver "chemical accuracy" (within 1 kcalmol^{-1}) in comparison with the G2/97 test set of reactions,[32,33] and has recently been shown to be successful for the calculation of the electrode potentials of cyclic nitroxide radical species,[24,25] and the bond dissociation energies of TEMPO-based alkoxyamines.[23,26] For reactions involving larger species, our *ab initio* version[23,34] of Morokuma's ONIOM method[35] was used to approximate G3-(MP2)-RAD calculations. In ONIOM, a chemical reaction is divided into a core section, which includes the reaction center and principal substituents, calculated at a high level of theory, and an outer section, which is the rest of the chemical system and is calculated only at a lower level. In forming the core section hydrogen atoms are included so that the correct valency is maintained and the core provides a good model of the chemical reaction. The energy of the full reaction is then obtained as the sum of the high level energy for the core system, and the substituent effect of the outer section calculated at the lower level. For the larger reactions in this study the core system, calculated at G3(MP2)-RAD, included the reaction center, with the piperidine ring structure truncated to $(CH_3)_2N-$ and in some cases the polymeric radical fragment $R- = -CH(CH_3)(OCOCH_3)$ truncated to $-CH_2(OCOH)$. The full system was calculated at RMP2/6-311+G(3df,2p)//B3-LYP/6-31G(d).

To calculate free energies of activation ($\Delta G^{\ddagger}$) and reaction (ΔG), entropies and thermal corrections were calculated using the standard textbook for formulas for the statistical thermodynamics of an ideal gas under the harmonic oscillator rigid rotor approximation in conjunction with the optimized geometries and scaled frequencies.[36] For kinetics calculations, the level of quantum-mechanical tunnelling was calculated using the Eckart method,[37] applied using G3(MP2)-RAD barriers and enthalpies and B3-LYP/6-31G(d) imaginary frequencies. The effective free energy barrier including tunnelling, $\Delta G_{\mathrm{eff}}^{\ddagger}$, was found from the equation $Q \exp(-\Delta G^{\ddagger}/RT) = \exp(-\Delta G_{\mathrm{eff}}^{\ddagger}/RT)$, where Q is the Eckart tunnelling coefficient. Where relevant, the free energy of solvation in an aqueous medium was added to the gas phase free energy of reactions. ΔG_{solv} was calculated using the polarized continuum models PCM[38] at the B3-LYP/6-31G(d) level as implemented in the GAUSSIAN 03 package. This approach has been previously shown to give accurate solvation energies in a study of the redox potentials of nitroxide radicals,[24] and in a study of the solution-phase equilibrium constants for the combination reactions of nitroxides and alkyl radicals.[26]

Scheme 2. Mechanisms for the Reaction between TEMPO−Alkoxyamine and Peroxyl Radical

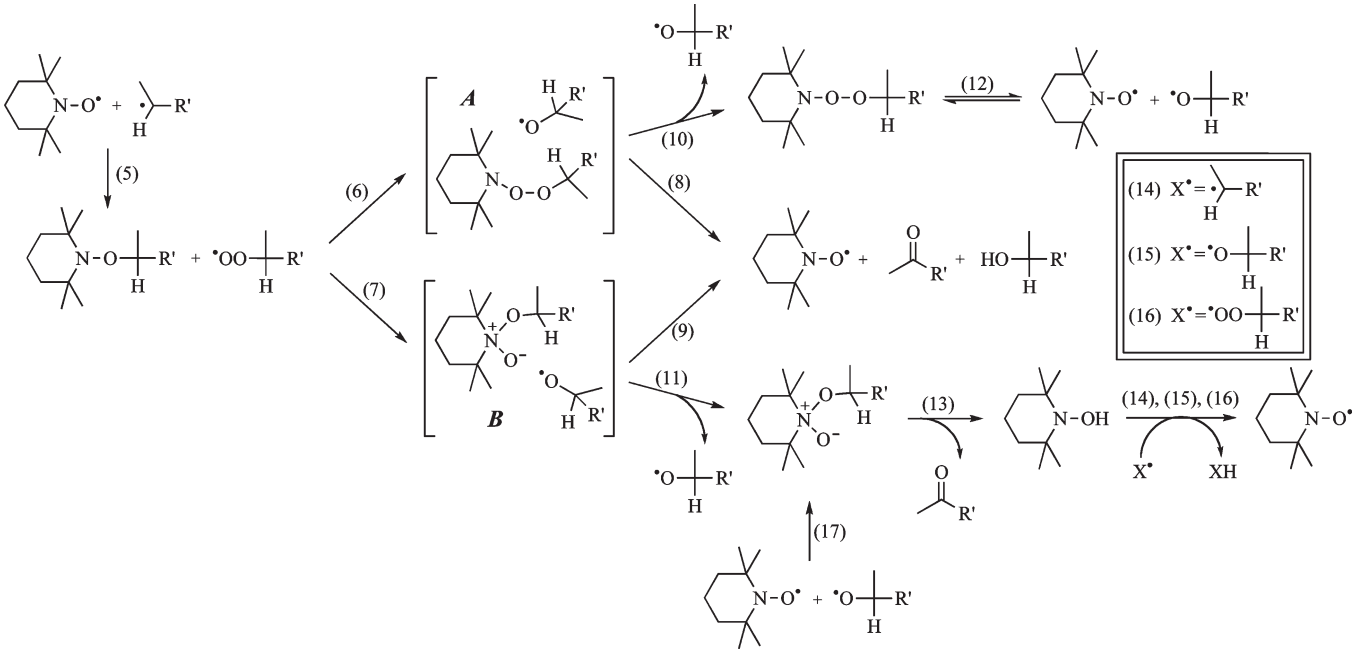

Where the charges and spin densities of intermediate and transition state species were useful in describing the structure of molecules, these were calculated using a NBO population analysis performed in GAUSSIAN at the B3-LYP/6-311+G(3df,2p) level.

Results

Table 1 shows the key thermodynamic parameters for all of the principal reactions and side reactions that have been attributed in the literature to the Denisov cycle (as shown in Schemes 2−4). In each case, these parameters were evaluated for R$^{\bullet}$ = $^{\bullet}$CH(CH$_3$)-(R′), R′ = CH$_3$, and R′ = OCOCH$_3$, which were chosen as small models of the typical mid chain radicals derived by hydrogen abstraction from two types of common polymer coatings, polyethylene and polyester.[39] The reactions were calculated at two different temperatures, room temperature (298.15 K) and 373.15 K (100 °C), to represent the upper limit of conditions undergone by polymer coatings used in roofing applications. On the basis of the free energies calculated from these reactions, the thermodynamically favorable reactions were identified and gas-phase free energy barriers for these reactions were then also calculated. The results of these calculations are shown in Table 2.

In this work, gas-phase reactions were considered, since they provide probably the best model of the polymer coating in a practical setting. However, as coatings may be solvated by water during weathering, the effects of an aqueous solvent on the thermodynamics of the reactions were also considered. The addition of an aqueous solvent to the calculations was found, in most cases, to cause an insignificant change to the thermodynamic results. However, for reactions involving the transfer of formal charges, the presence of an aqueous solvent provided a large stabilizing effect of around 500 kJ mol^{-1}. Therefore, the free energies for reactions (29) and (33) were calculated with the free energies of solvation in a water medium included in the calculations.

Discussion

Using the results in Tables 1 and 2 we can establish which reactions out of those collected in Schemes 2, 3 and 4 are most likely to contribute to the protection mechanism of polymer coating using HALS on the basis of their kinetics and thermodynamics. In what follows, we first examine those reactions proposed to contribute to the standard catalytic cycle (beginning with the combination of the polymeric radical and the nitroxide), before examining two large families of side reactions proposed to follow the combination of the peroxyl radical and the nitroxide, unimolecular decomposition of the resulting trioxide, and reaction of the trioxide with a secondary alcohol.

Standard Catalytic Cycle. Reaction 5 in Scheme 2, between the nitroxide 2,2,6,6-tetramethylpiperidin-1-yloxyl (TEMPO) and a polymeric radical, forms an alkoxyamine. Reactions of TEMPO with an alkyl radical make up the control reaction of TEMPO-based nitroxide mediated polymerization (NMP). These reactions are exothermic, having very fast rates of the order of 10^8 L mol^{-1} s^{-1}.[40,41] The calculated free energies of reaction 5 for the polyethylene and polyester model systems in this study, around −150 kJ mol^{-1}, indicate that the reaction forming a TEMPO-based alkoxyamine is very favorable. This reaction, like other very fast reactions that involve the combination of two radical species, is essentially barrierless.

The mechanism for the reaction of an alkoxyamine with a peroxyl radical has been studied using both computational and qualitative molecular orbital theory, and is now considered to proceed via a tetra-substituted nitrogen intermediate[5,13] or transition state,[15] which decomposes to form nitroxide, ketone and alcohol products as shown in reactions 8 and 9. Two different intermediates have been postulated on the basis of semiempirical computational studies[15,16] and molecular orbital arguments.[5] These intermediates are shown in the mechanisms described by reactions 6 and 7. The peroxyl radical adds to the alkoxyamine to form either an intermediate made up of an aminoperoxyether and an alkoxyl radical, labeled ***A***, or an intermediate made up of a zwitterionic oxyaminoether and an alkoxyl radical, labeled ***B***. These intermediate species have been prominent in previous literature discussions since they avoid the production of highly reactive and possibly polymer-damaging free alkoxyl radicals.[5] Although it has been suggested that reaction 7 may occur via a concerted process that regenerates the

Table 1. Thermodynamics Parameters for the Reactions shown in Schemes 2−4,[a]

	polyethylene (R′ = CH_3)						polyester (R′ = $OC(O)CH_3$)					
	298.15 K			373.15 K			298.15 K			373.15 K		
reaction	Δ*H* (kJ mol^{-1})	Δ*S* (J mol^{-1} K^{-1})	Δ*G* (kJ mol^{-1})	Δ*H* (kJ mol^{-1})	Δ*S* (J mol^{-1} K^{-1})	Δ*G* (kJ mol^{-1})	Δ*H* (kJ mol^{-1})	Δ*S* (J mol^{-1} K^{-1})	Δ*G* (kJ mol^{-1})	Δ*H* (kJ mol^{-1})	Δ*S* (J mol^{-1} K^{-1})	Δ*G* (kJ mol^{-1})
5	−212.8	−223.8	−146.1	−213.0	−224.4	−129.3	−234.7[b]	−219.1	−169.3	−234.7[b]	−219.3	−152.9
6	57.2[b]	−95.5	85.6	58.8[b]	−90.7	92.6	−36.8[c]	−100.5	−6.8	−34.9[c]	−95.1	0.5
7	−41.6[b]	−130.9	−2.5	−40.0[b]	−126.1	7.1	−99.1[c]	−143.8	−56.2	−97.7[c]	−139.4	−45.6
8	−367.5[b]	299.9	−456.9	−369.1[b]	295.1	−479.2	−299.2[c]	287.3	−384.9	−301.5[c]	280.6	−406.2
9	−268.7[b]	335.3	−368.7	−270.4[b]	330.4	−393.7	−236.9[c]	330.6	−335.4	−238.8[c]	325.0	−360.0
10	−47.9[b]	113.2	−81.6	−49.0[b]	109.9	−90.0	24.4[c]	121.9	−12.0	23.0[c]	117.8	−21.0
11	27.0[b]	131.0	−12.1	25.8[b]	127.5	−21.8	46.3[c]	145.5	2.9	45.2[c]	142.1	−7.9
12	60.7	187.0	5.0	34.5	10.6	30.5	11.7[b]	189.5	−44.8	11.1[b]	187.5	−58.9
13	−139.9	198.9	−199.2	−140.2	198.1	−214.1	−115.4[b]	192.1	−172.6	−116.7[b]	197.2	−190.3
14	−117.9	−15.8	−113.2	−118.7	−18.2	−111.9	−116.6	−3.9	−115.4	−117.3	−27.8	−115.0
15	−149.5	5.4	−151.1	−149.7	4.8	−151.5	−162.5	−6.9	−160.4	−162.9	−8.1	−159.8
16	−62.0	8.7	−64.6	−62.0	−49.3	−65.3	−81.7	−3.9	−80.6	−82.0	−4.5	−80.3
17	−106.7	−204.6	−45.7	−106.2	−203.1	−30.4	−125.9[b]	−209.3	−63.5	−125.3[b]	−207.5	−47.9
18	−12.6	−177.0	40.1	−11.8	−174.6	53.3	−39.4[b]	−190.3	17.4	−38.6[b]	−187.9	31.6
19	149.4	177.6	96.5	148.9	176.1	83.2	154.2[b]	195.7	95.9	153.7[b]	194.0	81.3
20	133.7	340.4	32.2	133.0	338.4	6.7	146.6[b]	358.5	39.7	145.9[b]	356.3	12.9
21	−196.1[b]	−183.2	−141.4	−195.2[b]	−174.3	−130.2	−196.1[b]	−183.2	−141.4	−195.2[b]	−174.3	−130.2
22	−102.1[b]	−190.6	−45.2	−101.3[b]	188.2	−31.0	−120.9[b]	−188.5	−64.7	−109.1[b]	−100.2	−71.7
23	−91.1[b]	333.6	−190.5	−92.4[b]	323.2	−213.0	−91.1[b]	333.6	−190.5	−92.4[b]	323.2	−213.0
24	−49.0[b]	341.7	−150.8	−50.0[b]	338.7	−176.4	−51.3[b]	344.3	−154.0	−52.4[b]	341.0	−179.7
25	−196.7	−198.6	−137.5	−170.5	−22.5	−162.2	−176.4[b]	−196.5	−117.8	−164.8[b]	−109.1	−124.1
26	10.0	12.3	6.3	10.4	13.5	5.3	8.6	0.5	8.5	9.0	1.6	8.4
27	130.8[b]	−22.5	137.5	131.0[b]	−21.8	139.2	136.3[b]	−6.1	138.1	136.5[b]	−5.5	138.5
28	−209.7[b]	146.6	−253.4	−210.6[b]	144.0	−264.3	−226.4[b]	146.7	−270.1	−227.2[b]	144.4	−281.0
29	567.4	159.6	44.7[d]	566.7	157.6	36.9[d]	501.8[b]	150.0	−6.1[d]	501.0[b]	147.5	−14.6[d]
30	−6.5	−24.3	0.7	−6.6	−24.4	2.5	−5.8[b]	−15.9	−1.1	−5.9[b]	−16.0	0.1
31	−146.4	174.6	−198.5	−146.7	173.7	−211.6	−121.2[b]	176.2	−173.7	−121.6[b]	174.9	−186.9
32	14.0	−198.7	73.2	14.6	−196.8	88.1	9.8[b]	−209.2	72.2	10.4[b]	−207.5	87.8
33	−727.8	213.7	−371.8[d]	−728.1	212.9	−380.7[d]	−632.9[b]	235.3	−309.2[d]	−633.0[b]	234.9	−318.6[d]

[a] G3(MP2)-RAD//B3-LYP/6-31G(d) values except where noted. [b] ONIOM approximation found using G3(MP2)-RAD core systems, $(CH_3)_2NO-$ in place of the TEMPO ring structure, with the full system calculated at RMP2/6-311+G(3df.2p). [c] ONIOM approximation found using G3(MP2)-RAD core systems, $(CH_3)_2NO-$ in place of the TEMPO ring structure and $R = CH_2OC(O)H$ in place of the $R = CH(CH_3)OC(O)CH_3$ polymeric fragment, with the full system calculated at RMP2/6-311+G(3df.2p). [d] Includes PCM solvation free energies at the B3-LYP/631G(d) level for an aqueous medium.

Table 2. Kinetic Parameters for the Thermodynamically Favorable Reactions shown in Scheme 2−4,[a]

	polyethylene ($R' = CH_3$)						polyester ($R' = OC(O)CH_3$)					
	298.15 K			373.15 K			298.15 K			373.15 K		
reaction	$\Delta H^‡$ (kJ mol^{-1})	$\Delta S^‡$ (J mol^{-1} K^{-1})	$\Delta G_{eff}^‡$ (kJ mol^{-1})^b	$\Delta H^‡$ (kJ mol^{-1})	$\Delta S^‡$ (J mol^{-1} K^{-1})	$\Delta G_{eff}^‡$ (kJ mol^{-1})^b	$\Delta H^‡$ (kJ mol^{-1})	$\Delta S^‡$ (J mol^{-1} K^{-1})	$\Delta G_{eff}^‡$ (kJ mol^{-1})^b	$\Delta H^‡$ (kJ mol^{-1})	$\Delta S^‡$ (J mol^{-1} K^{-1})	$\Delta G_{eff}^‡$ (kJ mol^{-1})^b
6	234.9^c	−169.4	285.4	236.0^c	−166.1	298.0	103.1^d	−190.1	159.1	104.1^d	−187.2	174.0
7	108.9^c	−177.7	160.2	109.8^c	−175.1	175.1	96.6^{d,e}	−199.7	154.5	97.5^{d,e}	−197.3	171.1
9	26.6^c	−21.9	28.9	26.3^c	−22.6	31.4	59.0^d	−49.0	70.7	58.8^d	−49.4	75.3
13	21.6	−0.3	20.8	21.3	−1.0	21.1	21.2^c	−6.3	21.7	21.0^c	−7.1	22.6
14^f	24.2^c	−43.1	31.5	23.4^c	−45.5	35.3	26.1^c	−25.5	28.9	25.4^c	−27.8	32.1
15^f	3.3^c	−7.6	5.5	2.8^c	−9.1	6.1		barrierless			barrierless	
16^f	25.6^c	−47.5	38.8	25.0^c	−49.3	42.6	7.5^c	−42.9	20.2	6.9^c	−44.8	23.5
26	54.0	−166.5	84.8	54.8	−164.2	103.5	37.7^c	−170.3	71.8	38.5^c	−167.9	89.4
30	54.3^c	−173.8	106.0	54.6^c	−172.7	119.0	21.4^d	−190.0	78.1	21.9^d	−188.5	92.3
31	99.9^c	−148.8	139.1	100.8^c	−146.0	152.2	72.1^d	−164.2	114.1	73.2^d	−160.8	128.3

[a] G3(MP2)-RAD//B3-LYP/6-31G(d) values except where noted. [b] Free energy barrier corrected for the effects of tunnelling. [c] ONIOM approximation found using G3(MP2)-RAD core systems, $(CH_3)_2NO-$ in place of the TEMPO ring structure, with the full system calculated at RMP2/6-311+G(3df,2p). [d] ONIOM approximation found using G3(MP2)-RAD core systems, $(CH_3)_2NO-$ in place of the TEMPO ring structure and $R = CH_2OC(O)H$ in place of the $R = CH(CH_3)OC(O)CH_3$ polymeric fragment, with the full system calculated at RMP2/6-311+G(3df,2p). [e] UMP2 calculation substituted for ROMP2 calculations in the G3(MP2)-RAD composite procedure due to convergence problems. [f] Determined in relation to the reaction going from a precomplex species to the transition state.

nitroxide radical via a six-membered ring transition state,[15] an intrinsic reaction coordinate (IRC) calculation performed as part of a previous theoretical study found that the reaction occurs via a stepwise mechanism.[16]

Nitroxide, ketone and alcohol products are formed from intermediates ***A*** and ***B*** through the hydrogen-transfer processes shown in reactions 8 and 9. It should be noted that, in the case that the two R′ groups are not the same, different ketone and alcohol products are produced. Previous labeling studies have found that, for reactions with a cyclohexyl peroxyl radical, the only products observed were those reached via intermediate ***B*** through reaction 9.[5,13]

In this work calculations confirm that the products of reactions 6 and 7 exist as the intermediate species ***A*** and ***B***, respectively. Examining the free energies calculated for reactions 6 and 7, it is clear that reaction 7 is thermodynamically more favorable; the formation of the intermediate exhibiting free energies of −2.5 and −56.2 kJ mol^{-1} for the polyethylene ($R' = CH_3$) and polyester radicals ($R' = OCOCH_3$) model systems respectively at 298.15 K and 7.1 and −45.6 kJ mol^{-1} respectively at 373.15 K. The formation of intermediate ***A*** is thermodynamically unfavorable at 298.15 K for the polyethylene system with a free energy of 85.6 kJ mol^{-1}, but is slightly exoergic, with a free energy of −6.8 kJ mol^{-1}, for the polyester system. Despite being a stationary point on the reaction energy surface it is clear that intermediate ***A*** is a much less stable species than intermediate ***B***, around 100 kJ mol^{-1} less stable for the polyethylene model system and around 60 kJ mol^{-1} less stable for the polyester model system. In the case of polyethylene this species exists in a very shallow potential well on an uphill pathway and is therefore not expected to form. An NBO population analysis on the species ***A*** and ***B*** was used to locate the charges and lone electrons within the molecules, the locations of which are shown in Scheme 2. It should be noted that while an intermediate species that resembles ***B*** has been postulated previously, the negative charge and lone electron in this previous description were located on different oxygen atoms.[5,13] The spin density of the lone electron in intermediate ***B*** was found to be located entirely on the separated alkoxyl radical species instead of on the nitrogen-bound oxygen.

From the calculated kinetic data, shown in Table 2, it is observed that the barriers for reaction 7 are similar for both polymer systems examined in this work; both free energy barriers are close to 160 kJ mol^{-1}. Of the barriers for reaction 6, only those of the polyester system are of similar magnitude at 159.1 kJ mol^{-1} at 298.15 K and 174.0 kJ mol^{-1} at 373.15 K. However, the barriers for the polyethylene system, at 285.4 kJ mol^{-1} at 298.15 K and 298.0 kJ mol^{-1} at 373.15 K, are much larger. The lower barrier for forming intermediate ***A*** in the case that the relevant polymer is a polyester derivative may be due an anomeric effect similar to that previously observed for similar alkoxyamines[26,42] stabilizing the transition state structure. Along with the thermodynamic evidence, this suggests that the mechanism proceeds through intermediate ***A*** for the polyester system but does not proceed in the case of the polyethylene system.

Reactions 8 and 9 are hydrogen atom transfer reactions within intermediates ***A*** and ***B*** that reform the nitroxide radical and generate ketone and alcohol products. These reactions are both very exoergic and are expected to take precedence over the competing reactions 10 and 11. If two different R′ groups are present, different ketone and alcohol products will be produced by reactions 8 and 9. For the case of polyethylene, the formation of intermediate ***A*** is thermodynamically unfavorable. The hydrogen atom transfer with-

in intermediate ***B***, in which the alkoxyl radical abstracts a methine hydrogen atom, is consistent with previous findings that only products reached through reaction 9 are formed.[5,13] However, for the polyester radical, the formation of intermediate ***A*** is thermodynamically favored and therefore contribution from reaction 8 is expected. For the polymeric radicals examined in this study, this reaction gives identical products to reaction 9.

A transition state structure could not be located for reaction 8, specifically for the polyester model system. Because of the very high exothermicity of this reaction, it is expected that the reaction is close to barrierless and displays a fast rate. The polyethylene and polyester systems exhibit low free energy barriers for reaction 9. These barriers were calculated to be 28.9 and 70.7 kJ mol^{-1} at 298.15 K, and 31.4 and 75.3 kJ mol^{-1} at 373.15 K, respectively, and imply rapid rates of reaction.

It is also possible that the intermediate species ***A*** and ***B*** may each dissociate, forming two discrete products, an alkoxyl radical species along with aminoperoxyether and oxyaminoether-type products, respectively. The alkoxyl radical is a highly reactive species that, if formed, may contribute to the propagation of the polymer degradation process. In various works, reactions involving the degradation of the aminoperoxyether or oxyaminoether products of reactions 10 and 11 have been postulated. The aminoperoxyether species may dissociate into the nitroxide and alkoxyl radical products shown in reaction 12.[17] It has been suggested that the oxyaminoether species may undergo an intramolecular hydrogen transfer reaction to yield a hydroxylamine and a ketone as shown in reaction 13.[18] In a previous study of the antioxidant activity of nitroxides in the inhibition of lipid peroxidation, it was postulated that hydroxylamines can donate hydrogen to alkyl, alkoxyl and peroxyl-type radicals forming nitroxide radicals.[43] Reactions 14, 15, and 16 show how hydroxylamine may detoxify alkyl and peroxyl radicals formed directly by the photo-oxidative degradation of polymer chains, as well as alkoxyl radicals formed by reactions 10 and 11.

Reactions 10 and 11 in Scheme 2 show the dissociation of intermediates ***A*** and ***B*** in which loss of an alkoxyl radical generates either a free aminoperoxylether or a free oxyaminoether, respectively. Reaction 10 is highly exothermic for the polyethylene model system showing a free energy of −81.6 kJ mol^{-1} at 298.15 K and −90.0 kJ mol^{-1} at 373.15 K. This is due to the instability of intermediate ***A*** in this case and also to the effects of entropy on forming two products from the intermediate complex. Intermediate ***A*** is only expected to form for the polyester system and, since reaction 10 is thermodynamically favored in this case (showing a free energy of −12.0 kJ mol^{-1} at 298.15 K and −21.0 kJ mol^{-1} at 373.15 K), formation of the aminoperoxylether species is expected to occur. Because of the large negative free energy of reaction 8, reaction 10 is likely to take place only to a small extent. The formed aminoperoxylether species dissociates through reaction 12 with free energies of −44.8 kJ mol^{-1} at 298.15 K and −58.9 kJ mol^{-1} at 373.15 K. In this reaction, the nitroxide and an alkoxyl radical are reformed. For the polyethylene model system it is expected that the reverse of reaction 12 may occur; that is, a nitroxide could react directly with any alkoxyl radical generated. However, the addition of a second alkoxyl radical to form intermediate ***A*** through the reverse of reaction 10 is not thermodynamically favorable.

Intermediate ***B*** exhibits a thermodynamically favored dissociation reaction for the polyethylene system and the polyester system at higher temperatures. At room temperature, the reaction in the polyester system is almost thermodynamically neutral. The free energies calculated for reaction 11 are −12.1 and 2.9 kJ mol^{-1} at 298.15 K and −21.8 and −7.9 kJ mol^{-1} at 373.15 K, respectively. Therefore, it is expected that a small amount of intermediate ***B*** will dissociate and produce the oxyaminoether species shown. Any free oxyaminoether is expected to rapidly undergo the intramolecular hydrogen transfer reaction to form hydroxylamine and ketone products, shown in reaction 13. This reaction is very favorable, with free energies of −199.2 and −172.6 kJ mol^{-1}, and low barriers of 20.8 and 21.7 kJ mol^{-1} for the polyethylene and polyester systems at 298.15 K, becoming even more favorable at higher temperatures.

It is expected that an oxyaminoether species may potentially be formed through the direct reaction of the nitroxide with any alkoxyl radical present in a reaction competing with the reverse of reaction 12 discussed above. This addition is depicted in reaction 17 and forms a zwitterionic oxyaminoether species. Thermodynamic parameters of this reaction show that it is more favorable than the reverse of reaction 12, in which nitroxide and alkoxyl radicals combine to form an aminoperoxylether species. Therefore, reaction 17 is expected to be the dominant reaction of nitroixde and alkoxyl radical species and will lead to the production of hydroxylamine and ketone species through the subsequent reaction 13. In this way nitroxides are also expected to directly consume polymer damaging alkoxyl radicals.

Reactions 14−16 were also calculated to be thermodynamically favorable. These results indicate that the nitroxide species will likely be reformed from a hydroxylamine via these reactions. Meanwhile, various polymeric carbon and oxygen-centered radicals are consumed. Reactions 14−16 were found to pass through various precomplex species prior to the transition state. A transition state was not located for reaction 15 for the polyester model system. The free energy barrier for this reaction is expected to be lower than that of the polyethylene system due to anomeric stabilization. Therefore, since the barrier for the polyethylene model system is only 5.5 kJ mol^{-1} at 298.15 K and 6.1 kJ mol^{-1} at 373.15 K, it is expected that reaction 15, for the polyester system, is essentially barrierless.

Trioxide Decomposition. The proposed Denisov cycle mechanism (Scheme 1) indicates that a nitroxide radical reacts with an alkyl radical $R^{\bullet}$ to form an alkoxyamine (reaction 5), which subsequently reacts with and detoxifies a peroxyl radical $ROO^{\bullet}$. However, it has been noted that while the reaction of the nitroxide and $R^{\bullet}$ is a fast reaction (exhibiting rate constants around 10^8 L mol^{-1} s^{-1}) the reaction between $R^{\bullet}$ and O_2 (reaction 3) is even faster. Rate constants for the latter reaction are typically an order of magnitude higher. On kinetic grounds, for the case where $R^{\bullet}$ = benzyl, less than 10% of the alkyl radicals that appear following the initiation of photodegradation are trapped by TEMPO,[19] and the subsequent reaction of the alkoxyamine with a peroxyl radical is expected to be slow. However, the experimental consumption and regeneration of TEMPO occurs at a higher rate than this suggests, implying that nitroxides also react directly, and catalytically, with peroxyl radicals, thereby transforming them into nonradical products. While this reaction is slower than the combination of two peroxyl radicals, it is likely to be competitive due to the high concentrations of nitroxide and low concentrations of peroxyl radicals present.[19]

Depicted in Scheme 3 are several reactions, drawn from the literature, which describe the combination of a nitroxide and a peroxyl radical and the subsequent decomposition of the product species. Several workers, implementing experimental and theoretical results, have suggested various

Scheme 3. Mechanisms for Degradation of the Trioxide Species

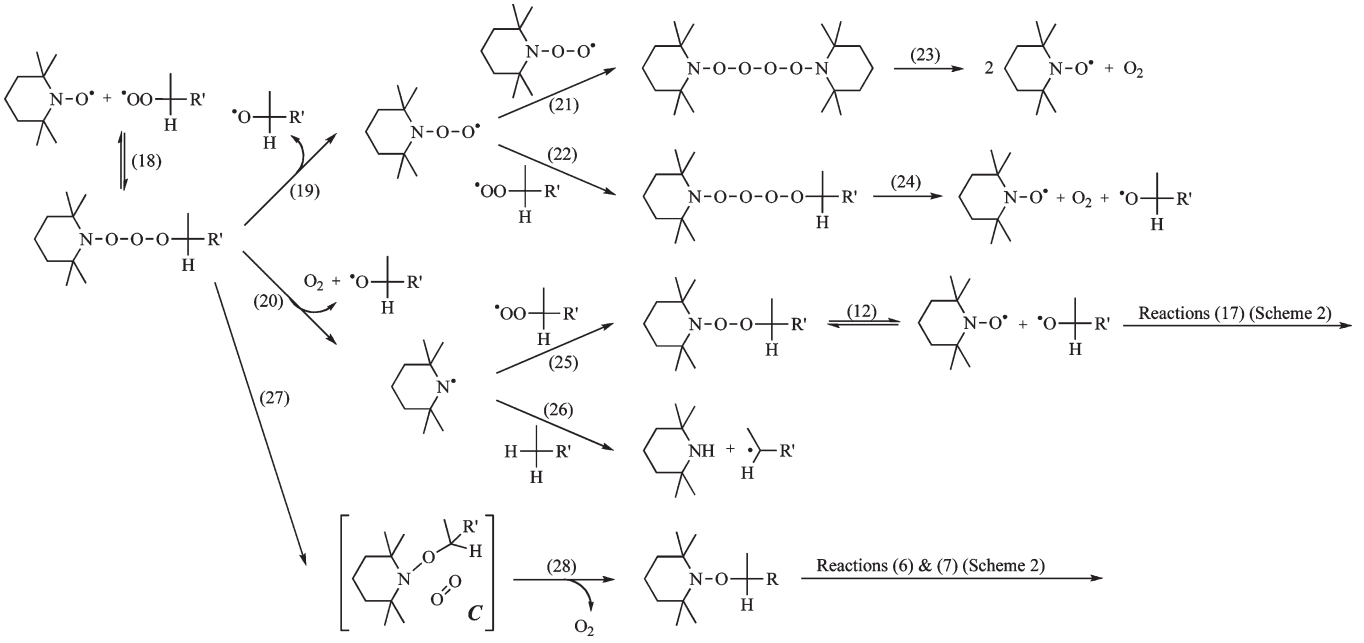

conflicting mechanisms and products for these reactions. The combination of the nitroxide and the peroxyl radical, shown in reaction 18, is generally agreed to give the trioxide species >N−O−O−O−R, first reported by Barton and coworkers.[17] It has been suggested that this species decomposes to radical products. Several different mechanisms for this process are listed in Scheme 3. It may be the case that the trioxide dissociates into an aminoperoxyl radical and an alkoxyl radical, shown in reaction 19, or an aminyl radical, dioxygen and an alkoxyl radical, shown in reaction 20. Further reactions with peroxyl and other radicals go on to regenerate nitroxide radicals, as shown in reactions 21−25.[17] The aminyl radical was also proposed to abstract a hydrogen atom, thereby forming an amine as shown in reaction 26.[17] Separately, it has been suggested that a concerted reaction may occur on the trioxide itself forming amine ketone and dioxygen products.[19] An intramolecular transfer reaction, shown in reactions 27 and 28, in which oxygen is released from the trioxide to deliver an alkoxyamine, was proposed by a thermochemical study[14] and was suggested to involve an intermediate species[19] labeled ***C***. However, this reaction is inconsistent with an experimental study in which no alkoxyamine product was detected.[17]

The reaction of TEMPO with a peroxyl radical, shown as reaction 18 in Scheme 3, exhibits a free energy of 40.1 kJ mol^{-1} for the polyethylene model system and 17.4 kJ mol^{-1} for the polyester model system at 298.15 K, increasing to 53.3 kJ mol^{-1} and 31.6 kJ mol^{-1} at 373.15 K. As expected, the reaction is exothermic due to the combination of two radicals to form a closed-shell species. However, the loss of translational entropy that takes place when two molecules combine causes a positive change in the free energy of the system. Reaction 18 becomes slightly more favorable as the reaction temperature is lowered, with the free energies for the polyethylene and polyester systems lowering to 35.7 kJ mol^{-1} and 12.6 kJ mol^{-1} at 273.15 K (0 °C). While on thermodynamic grounds this reaction is not expected to proceed, experimental studies have suggested that TEMPO does react with peroxyl radicals in small amounts. These results are based on the rate of consumption of TEMPO.[17,20] A driving force for the reaction may be the consumption of the formed trioxide species. Therefore, at such high concentrations of nitroxides, as are typically present in a HALS-protected polymer coating, it is expected that reaction 18 may contribute to the protection process demonstrated by HALS.

The degradation of the trioxide species by various suggested mechanisms is shown in Scheme 3. It has been suggested that decomposition of the trioxide into radical products takes place through homolytic cleavage of the oxygen−oxygen or nitrogen−oxygen bonds, as shown in reactions 19 and 20. Table 1 shows that reaction 19 is thermodynamically unfavorable. Calculated free energies for this reaction are 96.5 and 95.9 kJ mol^{-1} at 298.15 K and 83.2 and 81.3 kJ mol^{-1} at 373.15 K, for the polyethylene and polyester systems. Some reactions, drawn from the literature, suggest various other pathways for decomposition of the products of reaction 19. These pathways are represented by reactions 21−24. Although these reactions are thermodynamically favored, the thermodynamic constraints upon reaction 19 render these subsequent reactions unlikely. Reaction 20 is more entropically favorable, with free energies of 32.2 and 39.7 kJ mol^{-1} at 298.15 K, dropping to 6.7 and 12.9 kJ mol^{-1} at 373.15 K. It is clear that at high temperatures, reaction 20 is almost thermoneutral and may occur in small amounts, leading to the formation of aminyl radicals. Once formed the aminyl radical will readily abstract a hydrogen atom.[17] Because of its high concentration hydrogen abstraction will most likely occur from the polymer chain resulting in the formation of an R$^{\bullet}$ radical. This process, depicted in reaction 26 is almost thermoneutral and has free energy barriers of 84.8 and 71.8 kJ mol^{-1} at 298.15 K for the polyethylene and polyester model systems, increasing with higher temperatures. Therefore, the production of the amine 2,2,6,6-tetramethylpiperidine through this reaction is likely to occur to only a small extent. However, if it does occur, this side reaction will contribute to consumption of the nitroxide protecting agent, transforming it back to an amine HALS type species. Alternatively, the aminyl radical may extract hydrogen from a number of other closed-shell and radical present in thermodynamically favorable reactions, with rates dependent upon the relative concentrations of these species. For example, addition of a peroxyl

radical will generate aminoperoxylether as shown in reaction 25. As discussed above, in the case of the polyester system this species is expected to dissociate trough reaction 12 into nitroixde and alkoxyl products which may then subsequently react through reactions 17 and 13 and reactions 14, 15, or 16.

It has also been previously suggested that the trioxide species, formed with a secondary alkylperoxyl radical, may undergo a reaction analogous to the Russell mechanism,[44] in which the self-reaction of two secondary alkylperoxyl radicals liberates dioxygen, alcohol, and a ketone. This process would involve a concerted process on the trioxide, with a six-membered ring transition state transferring a hydrogen atom is to the nitrogen center.[19] Although this reaction is thermodynamically favorable, a transition state for the concerted reaction was not located. Systematic and exhaustive searching of the potential energy surface led instead to a five-membered ring transition state for a similar, but thermodynamically disfavored, reaction. This result implies that the concerted reaction does not occur.

The decomposition of the aforementioned trioxide into oxygen and an alkoxyamine through intermediate ***C*** was found to be thermodynamically unfavorable; reaction 27 exhibited free energies of 137.5 and 138.1 kJ mol^{-1} at 298.15 K for the polyethylene and polyester systems, with similar energies at 373.15 K. As such, it is unlikely that decomposition of the trioxide occurs via this mechanism. Notably, intermediate ***C*** was found to comprise an alkoxyamine and a dioxygen species. Conversely, the previously described intermediate was thought to comprise discrete aminyl and alkoxyl radicals with dioxygen.[19]

Trioxide Reaction with a Secondary Alcohol. More recently, it has been suggested that the decomposition of the trioxide species may occur via a reaction with a secondary alcohol. In the case that polymer coatings are protected from photo-oxidative damage, secondary alcohol is produced as one of the major products of the reaction between an alkoxyamine and a peroxyl radical (see reactions 8 and 9 in Scheme 2). The reaction between the trioxide and a secondary alcohol is reputed to proceed via the decomposition of the trioxide to the corresponding oxoammonium cation, appended by the functional group $>N^{+}{=}O$, and the reduced peroxyl anion ROO^{-}, shown in reaction 29.[20] The oxoammonium cation then proceeds to oxidize a secondary alcohol to form a ketone and hydroperoxide-type species, as well as the reduced form of the nitroxide, hydroxylamine $>N{-}OH$.[21] Two different mechanisms have been suggested for the reaction of the oxoammonium cation with an alcohol, both proceeding via a tetra-substituted nitrogen intermediate.[18,22] These reactions are shown as reactions 30 and 32 in Scheme 4, along with the concerted process, labeled reaction 31.

The reaction of the trioxide species with a secondary alcohol is thought to be preceded by an ionic fragmentation reaction that forms an oxoammonium cation and an anionic peroxyl species, shown in reaction 29. Thermodynamic parameters for the reaction, calculated on the trioxide in the gas phase, show that the reaction is extremely unfavorable. Enthalpies greater than 500 kJ mol^{-1} were calculated for both the polyethylene and polyester systems. However, this same calculation performed in an aqueous medium yielded free energies of 44.7 and -6.1 kJ mol^{-1} at 298.15 K and 36.9 and -14.6 kJ mol^{-1} at 373.15 K and for the polyethylene and polyester systems respectively, due to the stabilization of the charged species by the solvent. Reaction 29 is therefore only likely, at least for the polyester system, with the extra stabilization that an aqueous solvent provides. Although it is unclear to what extent polymer surface coatings are solvated during weathering, this reaction could potentially occur if water were present. In principle, formation of an oxoammonium cation may also occur through a self-disproportionation reaction of two nitroxide radicals. However, the gas-phase free energy calculated for this reaction was over 600 kJ mol^{-1} and the related free energy in an aqueous medium was calculated to be over 200 kJ mol^{-1}. This reaction is therefore unlikely to contribute to production of oxoammonium cations. The addition of a secondary alcohol to an oxoammonium cation forming a hydroxyaminoether-type species, as illustrated in reaction 32, is thermodynamically disfavored. Free energies of around 72 kJ mol^{-1} at 298.15 K and 88 kJ mol^{-1} at 373.15 K were calculated for the polyethylene and polyester systems. Reaction 32 is therefore unlikely to contribute to the overall protection mechanism, even if formation of the oxoammonium cation takes place.

The trioxide product species formed by reaction 18 exhibits a considerable elongation of the $>NO{-}OOR$ bond,

Scheme 4. Mechanisms for the Reaction between the Trioxide Species and a Secondary Radical

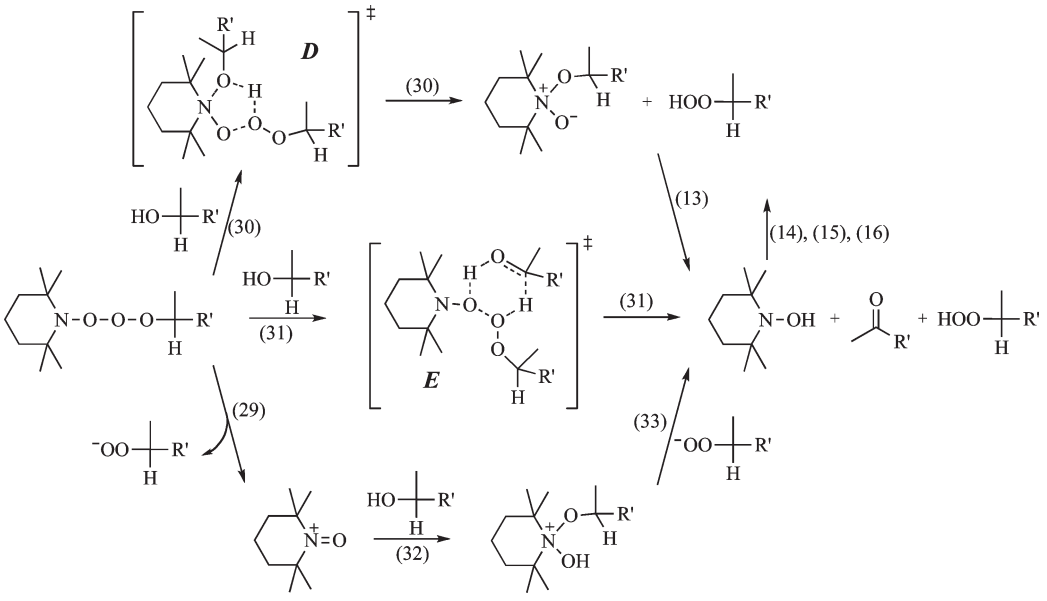

and this indicates an increased propensity for this bond to be cleaved during an ionic fragmentation process. The >NO−OOR bond length in the trioxide is 1.82 Å for the polyethylene model system and 1.86 Å for the polyester system. The distribution of charges within the trioxide molecule was investigated using a natural bond orbital (NBO) analysis.[45] In the ground state, the molecule was shown to contain significant charge separation, as shown in Figure 1, with partial positive charges of 0.23 and 0.29 on the nitroxyl fragment and −0.23 and −0.29 on the peroxyl fragment, for the polyethylene and polyester model systems, respectively. Therefore, in its lowest energy state, the trioxide exists as a partially dissociated molecule. It is likely that complete electron transfer is not required for attack by an electronegative oxygen to take place at the positive nitrogen center.

Reactions 30 and 31 describe the direct reaction of the trioxide with a secondary alcohol through either the five or six-membered ring transition states labeled ***D*** and ***E***. In reaction 30, the alcoholic oxygen adds to the nitrogen center, thereby transferring a hydrogen atom to the peroxyl fragment of the trioxide and forming an oxyaminoether and a hydroperoxide. The formed oxyaminoether then undergoes an intramolecular hydrogen transfer reaction 13 discussed previously. Reaction 30 was found to be an almost thermoneutral reaction with calculated free energy changes of 0.7 and −1.1 kJ mol^{-1} at 298.15 K and 2.5 and 0.1 kJ mol^{-1} at 373.15 K for the polyethylene and polyester systems. The free energy barriers of the reactions for the polyethylene and polyester systems were found to be 106.0 and 78.1 kJ mol^{-1}, respectively at 298.15 K, and are slightly higher at 373.15 K.

In reaction 31, both the alcoholic hydrogen atom and hydrogen atom on the adjacent carbon group are transferred, one to the nitroxide fragment and one to the peroxyl fragment, in a concerted reaction not previously described in literature. The six-membered ring transition state structure for the reaction is labeled as intermediate ***E*** in Scheme 4. From reaction 31, free energies of −198.5 and −173.7 kJ mol^{-1} and free energy barriers of 139.1 and 121.0 kJ mol^{-1} were calculated for the polyethylene and polyester systems respectively at 298.15 K. At the higher temperature of 373.15 K the free energies of the reactions become more negative by around 13 kJ mol^{-1}, while the barriers increased by a similar amount. It is therefore expected that reaction 31 will be the dominant reaction through which the trioxide reacts with secondary alcohols. The hydroxylamine, formed through reaction 31 may undergo subsequent reactions that convert it back to a nitroxide radical. These processes are described in the previously discussed reactions 14−16.

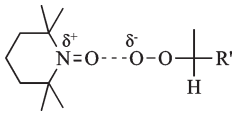

Figure 1. Partial positive and negative charges in the trioxide species.

Overall Process. On the basis of the results above we can now draw some conclusions about the primary reactions contributing to protection of polymer coatings by nitroxides, along with their most likely side reactions. These key reactions and their energetics for the reaction of TEMPO with radicals derived from the two different polymer coatings modeled in this study are summarized in Figures 2 and 3.

It is clear from Figures 2 and 3 that the dominant and catalytic mechanism of the Denisov cycle involves the addition of the nitroxide TEMPO to the polymeric radical R$^{\bullet}$ to form an alkoxyamine species, >N−OR. The alkoxyamine goes on to react with a peroxyl radical, thereby reforming the nitroxide along with ketone and alcohol products. For polyethylene systems, this process proceeds via an intermediate made up of a zwitterionic oxyaminoether and an alkoxyl radical, labeled ***B***. It should be noted that this mechanism is consistent the experimental observation that when the reaction between O-18 labeled nitroxide and cyclohexyl peroxyl radical occurs, a labeled oxygen is transferred to the ketone product.[5,13] A similar mechanism occurs for polyester systems; however, the reaction also proceeds, to a similar extent, through an intermediate made up of an aminoperoxyether and an alkoxyl radical, labeled ***A***. Small amounts of reactants that escape the intermediate "cage" also go on to regenerate nitroxide radicals. These primary mechanisms are consistent with the experimental observation that ketones and alcohols are produced by the reaction of nitroxides and alkylperoxyl radicals.[13]

TEMPO can also react with any free alkoxyl radicals that are present forming zwitterionic oxyaminoether species (>N^{+}(O^{-})−OR), which then undergoes an intramolecular hydrogen-transfer reaction to form the reduced form of TEMPO (the hydroxylamine >N−OH) and a ketone.

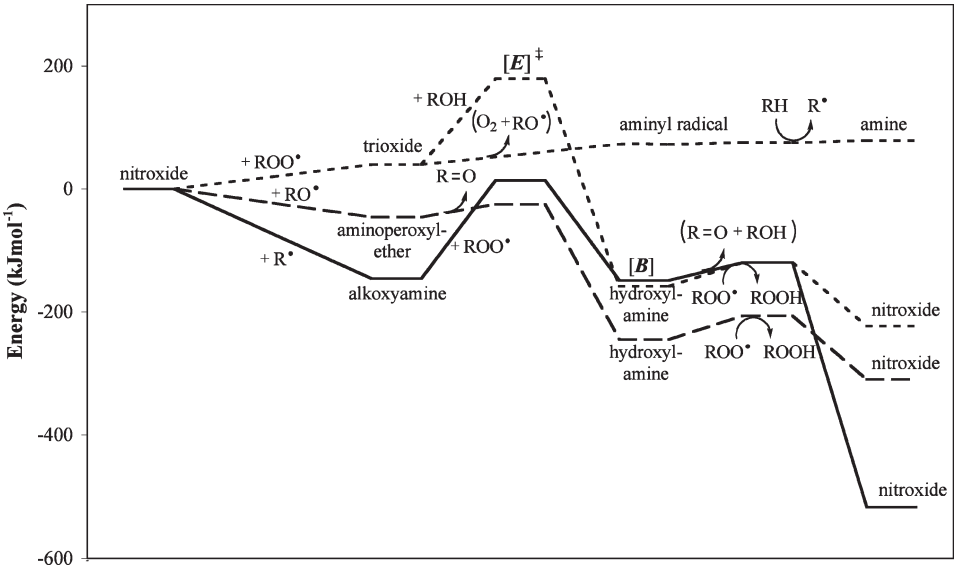

Figure 2. Normalized reaction energetics (298.15 K) for polyethylene.

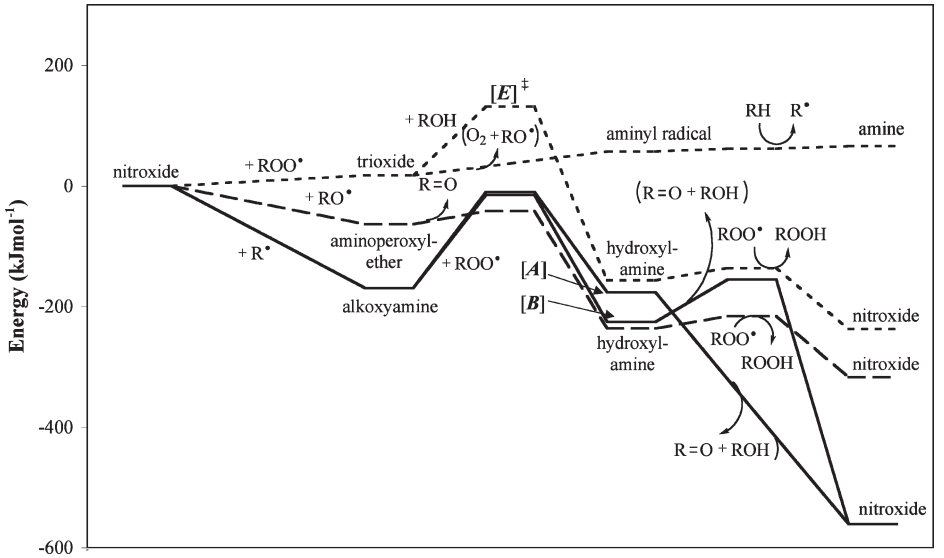

Figure 3. Normalized reaction energetics (298.15 K) for polyester.

Scheme 5. Major Products of the Reactions of Alkyl, Alkoxyl, and Peroxyl Radicals with TEMPO

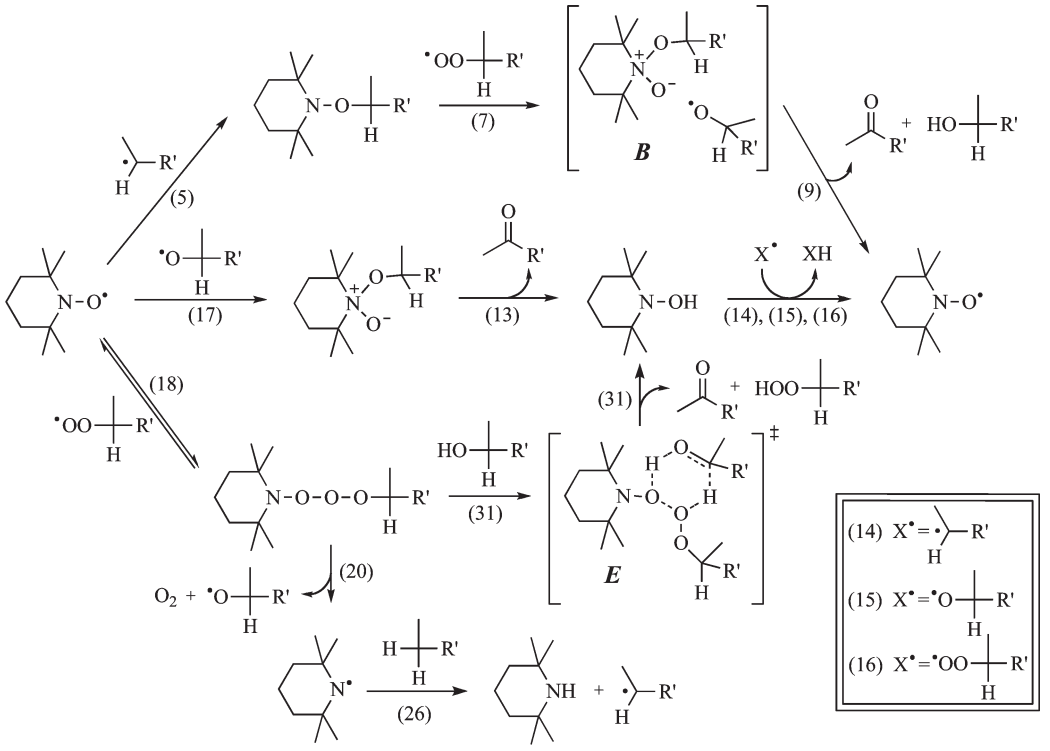

The corresponding nitroxide radical is regenerated from hydrogen-transfer from the hydroxylamine to an alkyl, alkoxyl, or peroxyl radical.

Another possible side reaction is the slower reaction between TEMPO and the peroxyl radical ROO•, however this reaction becomes less favorable as the temperature increases toward the types of conditions sometimes experienced by surface coatings in roofing applications. From this pathway, the trioxide species >N−O−O−O−R is formed. The trioxide may go on to react with the secondary alcohol product from the dominant pathway hydroxylamine >N−OH, a ketone and a hydroperoxide species via a concerted mechanism involving a six-membered ring transition state. A possible consuming side reaction for the nitroxide protecting agent is the trioxide decomposition into an aminyl radical, a hydroxyl radical, and dioxygen. Hydrogen donation to the aminyl radical may then form an amine HALS-type species. It is expected that a nitroxide will be regenerated from the amine through oxidation reactions (see Scheme 1); however, this side reaction may lead to greater than expected concentrations of HALS in the reaction medium.

Conclusions

The Denisov cycle describes the protection of polymer coatings from oxidative degradation caused by weathering effects, through the use of hindered amine light stabilizers (HALS). Previous mechanistic descriptions of this process have often been

incomplete or inaccurate. Through prior experimental and theoretical studies, around a dozen different reaction pathways comprising over 30 individual reactions have been proposed to contribute to the overall mechanism. The high-level quantum chemical study presented in this work discriminates, for the first time, between all the suggested reactions based on calculations of their kinetic and thermodynamic parameters. On the basis of this work, the preferred mechanism of the catalytic cycle and its most likely side reactions are summarized in Scheme 5.

Acknowledgment. We gratefully acknowledge generous allocations of computing from the Australian Partnership for Advanced Computing and the Australian National University Supercomputing Facility, support from the Australian Research Council under their Centres of Excellence program, and the award (to J.L.H.) of an Australian Postgraduate Award. We also thank Professor Steven Bottle, Dr Phillip Barker and the other members of the materials group of the ARC Centre of Excellence for Free Radical Chemistry and Biotechnology for their useful feedback on this work.

Supporting Information Available: Tables of B3-LYP/6-31G(d) optimized geometries in the form of GAUSSIAN archive entries and corresponding total energies. This material is available free of charge via the Internet at http://pubs.acs.org.

References and Notes

(1) Yebra, D. M.; Kill, S.; Dam-Johansen, K. *Prog. Org. Coat.* **2004**, *50*, 75.
(2) Allen, N. S. *Chem. Soc. Rev.* **1986**, *15*, 373.
(3) Denisov, E. T. *Dev. Poly. Degrad.* **1982**, *5*, 23.
(4) (a) Bolland, J. L. *Proc. R. Soc. London, A* **1946**, *186*, 218. (b) Bolland, J. L.; Gee, G. *Trans. Faraday Soc.* **1946**, *42*, 236. (c) Bolland, J. L.; Gee, G. *Trans. Faraday Soc.* **1946**, *42*, 244.
(5) Step, E. N.; Turro, N. J.; Klemchuk, P. P.; Gande, M. E. *Angew. Makromol. Chem.* **1995**, *232*, 65.
(6) Bortolus, P.; Camaioni, N.; Flamigni, L.; Minto, F.; Monti, S. *J. Photochem. Photobiol. A: Chem.* **1992**, *68*, 239.
(7) Pospísil, J. *Adv. Polym. Sci.* **1995**, *124*, 87.
(8) Gugumus, F. *Polym. Degrad. Stab.* **1993**, *40*, 167.
(9) Pospísil, J.; Pilar, J.; Nespurek, S. *J. Vinyl Add. Tech.* **2007**, *13*, 119.
(10) Pan, J.-Q.; Yan, S. *Polym. Degrad. Stab.* **1991**, *32*, 79.
(11) Carlsson, D. J.; Wiles, D. M. *Polym. Degrad. Stab.* **1984**, *6*, 1.
(12) Wiles, D. M.; Tovborg-Jesen, J. P.; Carlsson, D. J. *Pure Appl. Chem.* **1983**, *55*, 1651.
(13) Klemchuk, P. P.; Gande, M. E.; Cordola, E. *Polym. Degrad. Stab.* **1990**, *27*, 65.
(14) Stipa, P. *J. Chem. Soc., Perkin Trans. 2* **2001**, 1793.
(15) Kysel, O.; Mach, P.; Micov, M. *Polym. Degrad. Stab.* **1993**, *40*, 31.
(16) Rossi, I.; Venturini, A.; Zedda, A. *J. Am. Chem. Soc.* **1999**, *121*, 7914.
(17) Barton, D. H. R.; Le Gloahec, V. N.; Smith, J. *Tetrahedron Lett.* **1998**, *39*, 7483.
(18) Ma, Z.; Bobbitt, J. M. *J. Org. Chem.* **1991**, *56*, 6110.
(19) Schwetlick, K.; Habicher, W. D. *Polym. Degrad. Stab.* **2002**, *78*, 35.
(20) Goldstein, S.; Samuni, A. *J. Phys. Chem. A* **2007**, *111*, 1066.
(21) (a) Golubev, V. A.; Zhdanov, R. I.; Gida, V. M.; Rozantsev, E. G. *Bull. Acad. Sci. U.S.S.R., Chem. Ser.* **1971**, *20*, 768. (b) Ganem, B. *J. Org. Chem.* **1975**, *40*, 1998.
(22) Semmelhack, M. F.; Schmid, C. R.; Cortés, D. A. *Tetrahedron Lett.* **1986**, *27*, 1119.
(23) Izgorodina, E. I.; Brittain, D. B. R.; Hodgson, J. L.; Krenske, E. H.; Lin, C. Y.; Namazian, M.; Coote, M. L. *J. Phys. Chem. A* **2007**, *111*, 10754.
(24) Hodgson, J. L.; Namazian, M.; Bottle, S. E.; Coote, M. L. *J. Phys. Chem. A* **2007**, *111*, 13595.
(25) Blinco, J. P.; Hodgson, J. L.; Morrow, B. J.; Walker, J. R.; Will, G. D.; Coote, M. L.; Bottle, S. E. *J. Org. Chem.* **2008**, *73*, 6763.
(26) Hodgson, J. L.; Lin, C. Y.; Coote, M. L.; Marque, S. R. A.; Matyjaszewski, K. *Macromolecules* **2010**, *43*, 3728−3743.
(27) Hehre, W. J.; Radom, L.; Schleyer, P. V. R.; Pople, J. A. *Ab Initio Molecular Orbital Theory*; Wiley: New York, 1986.
(28) Koch, W.; Holthausen, M. C. *A Chemist's Guide to Density Functional Theory*; Wiley-VCH: Weinheim, Germany, 2000.
(29) Frisch, M. J.; Trucks, G. W.; Schlegel, H. B.; Scuseria, G. E.; Robb, M. A.; Cheeseman, J. R.; Montgomery, J. A., Jr.; Vreven, T.; Kudin, K. N.; Burant, J. C.; Millam, J. M.; Iyengar, S. S.; Tomasi, J.; Barone, V.; Mennucci, B.; Cossi, M.; Scalmani, G.; Rega, N.; Petersson, G. A.; Nakatsuji, H.; Hada, M.; Ehara, M.; Toyota, K.; Fukuda, R.; Hasegawa, J.; Ishida, M.; Nakajima, T.; Honda, Y.; Kitao, O.; Nakai, H.; Klene, M.; Li, X.; Knox, J. E.; Hratchian, H. P.; Cross, J. B.; Adamo, C.; Jaramillo, J.; Gomperts, R.; Stratmann, R. E.; Yazyev, O.; Austin, A. J.; Cammi, R.; Pomelli, C.; Ochterski, J. W.; Ayala, P. Y.; Morokuma, K.; Voth, G. A.; Salvador, P.; Dannenberg, J. J.; Zakrzewski, V. G.; Dapprich, S.; Daniels, A. D.; Strain, M. C.; Farkas, O.; Malick, D. K.; Rabuck, A. D.; Raghavachari, K.; Foresman, J. B.; Ortiz, J. V.; Cui, Q.; Baboul, A. G.; Clifford, S.; Cioslowski, J.; Stefanov, B. B.; Liu, G.; Liashenko, A.; Piskorz, P.; Komaromi, I.; Martin, R. L.; Fox, D. J.; Keith, T.; Al-Laham, M. A.; Peng, C. Y.; Nanayakkara, A.; Challacombe, M.; Gill, P. M. W.; Johnson, B.; Chen, W.; Wong, M. W.; Gonzalez, C.; Pople, J. A. *Gaussian 03, Revision B.03*; Gaussian, Inc.: Pittsburgh PA, 2003.
(30) Werner, H.-J.; Knowles, P. J.; Amos, R. D.; Bernhardsson, A.; Berning, A.; Celani, P.; Cooper, D. L.; Deegan, M. J. O.; Dobbyn, A. J.; Eckert, F.; Hampel, C.; Hetzer, G.; Korona, T.; Lindh, R.; Lloyd, A. W.; McNicholas, S. J.; Manby, F. R.; Meyer, W.; Mura, M. E.; Nicklass, A.; Palmieri, P.; Pitzer, R.; Rauhut, G.; Schütz, M.; Stoll, H.; Stone, A. J.; Tarroni, R.; Thorsteinsson, T. *MOLPRO 2000.6*; University of Birmingham: Birmingham, U.K., 1999.
(31) Scott, A. P.; Radom, L. *J. Phys. Chem.* **1996**, *100*, 16502.
(32) Henry, D. J.; Sullivan, M. B.; Radom, L. *J. Chem. Phys.* **2003**, *118*, 4849.
(33) Curtiss, L. A.; Raghavachari, K. *Theor. Chem. Acc.* **2002**, *108*, 61.
(34) Lin, C. Y.; Hodgson, J. L.; Namazian, M.; Coote, M. L. *J. Phys. Chem. A* **2009**, *113*, 3690.
(35) Humbel, S.; Sieber, S.; Morokuma, K. *J. Chem. Phys.* **1996**, *105*, 1959.
(36) (a) See for example Steinfeld, J. I.; Francisco, J. S.; Hase,W. L. *Chemical Kinetics and Dynamics*; Prentice Hall: Englewood Cliffs, NJ, 1989.(b) These formulas are outlined in full in the Supporting Information of an earlier publication in this journal: Coote, M. L.; Radom, L. *Macromolecules* **2004**, *37*, 590.
(37) (a) Eckart, C. *Phys. Rev.* **1930**, *35*, 1303. (b) For a description of this method, see, for example: Coote, M. L.; Collins, M. A.; Radom, L. *Mol. Phys.* **2003**, *101*, 1329.
(38) Goldstein, S.; Samuni, A.; Russo, A. *J. Am. Chem. Soc.* **2003**, *125*, 8364.
(39) (a) Lindsay Smith, J. R.; Nagatomi, E.; Stead, A.; Waddington, D. J.; Bévière, S. D. *J. Chem. Soc., Perkin Trans. 2* **2000**, 1193. (b) Lindsay Smith, J. R.; Nagatomi, E.; Waddington, D. J. *J. Chem. Soc., Perkin Trans. 2* **2000**, 2248. (c) Lindsay Smith, J. R.; Nagatomi, E.; Stead, A.; Waddington, D. J. *J. Chem. Soc., Perkin Trans. 2* **2001**, 1527.
(40) Sobek, J.; Martschke, R.; Fischer, H. *J. Am. Chem. Soc.* **2001**, *123*, 2849.
(41) Beckwith, A. L. J.; Bowry, V. W.; O'Leary, M.; Moad, G.; Rizzardo, E.; Solomon, D. H. *J. Chem. Soc., Chem. Comm.* **1986**, 1003.
(42) Gaudel-Siri, A.; Siri, D.; Tordo, P. *ChemPhysChem* **2006**, *7*, 430.
(43) Miura, Y.; Utsumi, H.; Hamada, A. *Arch. Biochem. Biophys.* **1993**, *300*, 148.
(44) (a) Russell, G. A. *J. Am. Chem. Soc.* **1957**, *79*, 3871. (b) Howard, J. A.; Ingold, K. U. *J. Am. Chem. Soc.* **1968**, *90*, 1056.
(45) Foster, J. P.; Weinhold, F. *J. Am. Chem. Soc.* **1980**, *102*, 7211.